# We are IntechOpen, the world's leading publisher of Open Access books Built by scientists, for scientists

**4,800**
Open access books available

**122,000**
International authors and editors

**135M**
Downloads

Our authors are among the

**154**
Countries delivered to

**TOP 1%**
most cited scientists

**12.2%**
Contributors from top 500 universities

CLARIVATE ANALYTICS BOOK CITATION INDEX INDEXED

WEB OF SCIENCE™

Selection of our books indexed in the Book Citation Index in Web of Science™ Core Collection (BKCI)

## Interested in publishing with us?
## Contact book.department@intechopen.com

Numbers displayed above are based on latest data collected.
For more information visit www.intechopen.com

Chapter 10

# Ion Exchange Fundamentals and New Challenges

Maria Angélica Simões Dornellas de Barros, Marcelino Luiz Gimenes, Melissa Gurgel Adeodato Vieira and Meuris Gurgel Carlos da Silva

Additional information is available at the end of the chapter

http://dx.doi.org/10.5772/60864

**Abstract**

Ion exchange is a stoichiometric phenomenon commonly used in water treatment as an end-of-pipe technique. Such process is highly influenced by mass transfer conditions and may be modeled by adsorption equations. Although widely applied in industries its theory has not been completely understood and depends on the exchanger characteristics. Moreover, competitive systems may add complexity and decrease removal efficiency and exchanger selectivity mainly in dynamic systems. In this chapter some general theory was presented and some detailed examples involving alginate biopolymer, bonechar and zeolite in single and competitive systems were discussed in batch and continuous state.

**Keywords:** ion exchange, kinetics, equilibrium data, fixed bed, multicomponent systems

## 1. Introduction

Ion exchange processes are the processes in which a solid phase (ion exchanger) reacts in a double exchange reaction when in contact with a liquid phase with electrolytes. Actually, this should not be considered as a true chemical reaction as it involves the redistribution of ions between two phases by diffusion. Chemical factors are almost negligible with small amount of heat, often less than 2 kcal/mol [1].

In an ion exchange process, the balancing ion (the one previously detected in the solid phase) is replaced by the counter ion (previously in the liquid phase) always when the exchange has a higher affinity to the counter ion. It is important to emphasize that the stoichiometric replacement involves charges. Nevertheless, normality is much more adequate to describe the phenomenon than molarity. Figure 1 presents examples of the monovalent and divalent exchange processes. In this diagram, it is easy to see the importance of charges in the stoichiometric process.

The first citation of an application of ion exchange can be found in Aristotle's, but the ion exchange processes became well known in the nineteenth century. In the 1930s, they were strengthened when organic cation exchangers were discovered. Nowadays, anion exchange resins are also commercially obtained [2].

Ion exchange is considered as an end-of-pipe technique used in wastewater and one of the best available techniques to remove heavy metal ions, which is of a great concern due to the toxic compounds constantly presented in bodies of water.

With such general aspects in mind, this chapter has the main goal to discuss the ion exchange phenomenon through already published results. Theory and fundamental aspects will be briefly revised.

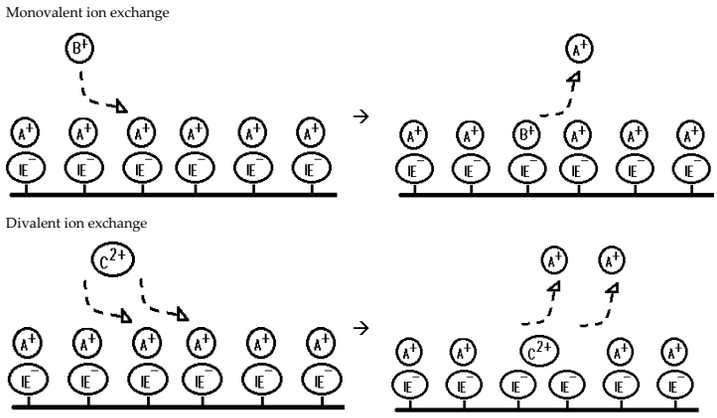


**Figure 1.** Cationic exchange examples. $IE^-$ is the ionic exchanger charge. A is the balancing cation, B is the monovalent counter ion, and C is the divalent counter ion.

## 2. General theory

Ion exchange is generally controlled by diffusion, a consequence of the material structure. Ion exchange framework, size of the beads, and any other physical chemistry characteristics have important roles in this process. Nevertheless, in all cases, it is accomplished by transfer of ions to and from the interphase boundary, the exchange itself followed by the diffusion of the ion inside the solid phase and the diffusion in the surrounding solution.

Actually, the ion exchange process occurs in the following steps [2]:

1. Dissociation of the electrolytes in the bulk phase, originating the denominated counter ion
2. Diffusion of the counter ion from the bulk phase towards the interphase film
3. Diffusion of the counter ion through the interphase film
4. Diffusion of the counter ion inside the ion exchanger

http://dx.doi.org/10.5772/60864

5. Association between the counter ion and the functional group of the exchanger
6. Dissociation of the balancing ion and functional group of the exchanger
7. Diffusion of the balancing ion inside the exchanger towards the surface
8. Diffusion of the balancing ion through the interphase film
9. Diffusion and random distribution of the balancing ion in the bulk phase
10. Formation of the balancing ion complexes in the solution

Basically, the mechanism of ion exchange processes has some possible rate-controlling steps. The most important ones are related to steps 3 and 8, 4 and 7, 5 and 6. Steps 3 and 8 deal with film resistance and should be minimized through adequate agitation. The mass transfer in this case is defined by the diffusion coefficients. Steps 4 and 7 are related to intraparticle diffusion and depend on the physic-chemical properties of the system. Small particles of the ion exchanger may decrease such resistances. Steps 5 and 6 are the ion exchange processes properly. Almost always, the film and/or intraparticle resistances are considered the most important rate-controlling steps. Many kinetic models take into account these characteristics. More information regarded to kinetics can be seen elsewhere [3, 4]. The regeneration of the saturated ion exchanger may be also modeled [5]. It must be emphasized that many models are used to describe both adsorption and ion exchange mechanisms. Despite of the mathematical similarity, the significant differences related to these mechanisms should be in mind.

Besides kinetic data, ion exchange equilibrium data are also of great value. Isotherms may be classified in five different types [6], as shown in Figure 2.

Isotherm shapes indicate whether or not the ion is solution is preferably exchanged. However, they provide no information on the type of exchange sites or even whether they have similar energies. This is outstanding information as it is directly related to the ion exchange mechanism. The Kielland plot is an interesting thermodynamic tool to understand such process. Ion selectivity and the thermodynamic properties may be obtained from such data.

The Kielland plot may be obtained through $\log K \mid_{B}^{A}$ (equilibrium constant through the balancing ion A and the counter ion B) and $x_{A(Z)}$. Linear Kielland plots are a consequence of exchangers with only one kind of exchange site [7]. Nonlinear plots indicate different sites and different cavities where the exchanged cation occupies different positions in the framework [6].

Although batch operations where isotherms may be obtained are rarely used in industries, they are very common when investigating mechanisms such as the ones in equilibrium through isotherms. Continuous systems are almost often well suited for industrial purposes when scale-up process is needed. Continuous ion exchange uses packed beds where the mass transfer is of great importance. As the feed solution passes through the ion exchange packed bed, the outlet solution has different concentrations of the incoming ion as a function of time. Plots of the ratio outlet concentration of the incoming ion/concentration of the incoming ion in the feed solution versus time are well known as breakthrough curve. Mass balances in the column as well as the mass transfer parameters are reported elsewhere [8,9].

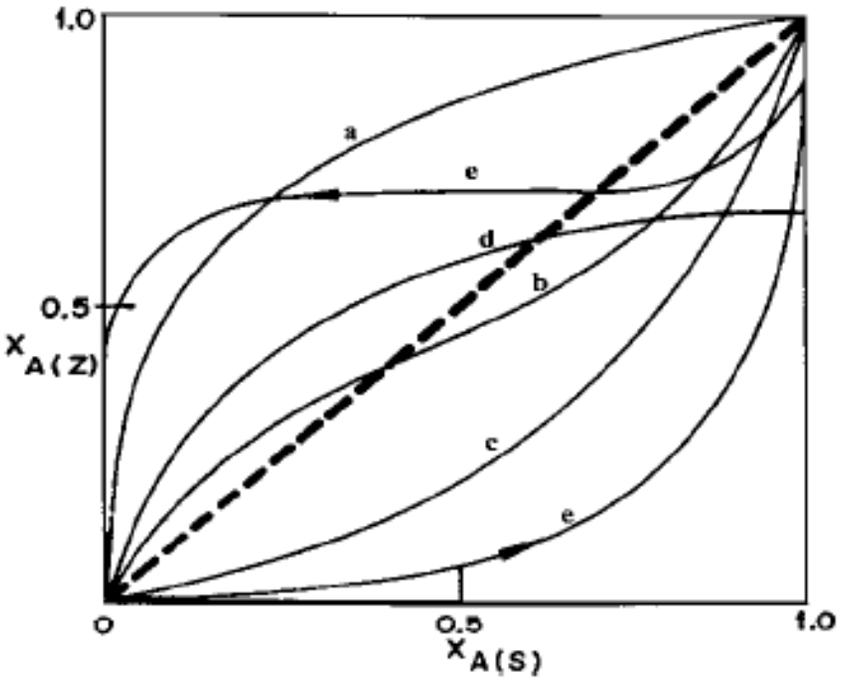


**Figure 2.** Ion exchange isotherms: $x_{a(z)}$: equivalent fraction of the counter ion in the exchanger; $x_{a(s)}$: equivalent fraction of the counter ion in solution [6]. (a) Favorable isotherm; (b) isotherm with reversal behavior, from favorable to unfavorable; (c) unfavorable isotherm; (d) incomplete favorable isotherm; (e) isotherm with hysteresis.

Besides the use of adsorption models, ion exchange systems may be more correctly represented by the mass action law (MAL). This is the most characteristic property of ion exchange and can be used as one of the possible modeling equations. Actually, it expresses the typical double exchange reaction where the balancing ion in the exchanger is replaced by the in-going ion according to the stoichiometry.

MAL is based on the definition of the chemical equilibrium of the chemical reactions first proposed by Cato Guldberg and Peter Waage in 1864. It was defined as the equilibrium constant *K*, which is the relationship of the activity coefficient of reagents and products in equilibrium at a given temperature.

If the chemical reaction presented in Eq. (1) is considered:

$$bB + cC \rightarrow dD + eE \tag{1}$$

The equilibrium constant may be written as follows:

$$K = \frac{\left[a_D\right]^d \cdot \left[a_E\right]^e}{\left[a_B\right]^b \cdot \left[a_C\right]^c} \tag{2}$$

http://dx.doi.org/10.5772/60864

where *a* stands for the ionic activity of each ion presented in Eq. (1).

It is obvious that monocomponent ion exchange only occurs when the solid in is contact with synthetic solutions. Other solutions, mainly wastewaters, always contain significant amount or other ions that may be also exchanged. That is why selectivity and affinity properties of the ion exchanger in relation to the specific incoming ion should be considered no matter if it is continuous or batch system. Of course, in such a case, modeling is more complex. Some examples of MAL can be seen in reference [10].

## 3. Ion exchangers

Ion exchangers are porous matrixes from different sources, with positive or negative excess charge, insoluble in aqueous solutions and in many organic solvents. The excess charge of the matrix should be compensated by the balancing ions, which may be replaced by the in-going ion depending on the selectivity and affinity of the exchanger to the ions involved.

Mechanical resistance as well as regeneration capacity is quite important when packed beds are considered. There are acid and basic exchangers being the anionic exchangers that have basic superficial groups and cationic exchangers those containing superficial acid groups. Exchangers may be also classified according to complete or incomplete dissociation based on the pH range where the exchange process is efficient.

Ion exchangers can be natural such as alginate, clay, algae, or even some zeolites. Alginate occurs in seaweeds as calcium alginate and is present in the cells of brown algae. Actually, the term alginate designates salts of alginic acid and its derivatives.

Clays are fine powders constituted by hydrated aluminosilicates that often tend to agglomerate. In clay materials alumina is presented in octahedral form whereas silica is found as tetrahedrons. Such materials are thermally stable and can be greatly improved by pillaring process. Zeolites are also aluminosilicates. Nevertheless, they have an open three-dimensional framework with interconnecting cavities. Both materials can be used as adsorbents, ion exchangers, catalysts, or catalysis support.

Natural exchangers have some disadvantages such as low exchange rate and rather poor mechanical properties and low abrasion resistance, which restrict their application, mainly in packed beds without any previous treatment.

Exchangers obtained specifically from synthetic materials are available commercially being. Zeolites and resins are the most famous representatives of such class. Many zeolites are related to cationic exchange process. Nevertheless, zeolites can act as anionic exchangers if tailored.

Resins are known since 1935. They can be used as ion exchangers or catalysts. Ion exchange resins may be found as in acids and bases, acting, therefore, as anionic or cationic exchangers. Cationic resins generally contain sulfonic acid groups, whereas anionic resins are commonly found in quaternary ammonium groups.

## 4. Experimental results of ion exchange

### 4.1. Case study: Metallic ion in calcium alginate biopolymer

*4.1.1. Copper kinetics study of calcium alginate particles in a static system*

Calcium alginate biopolymer was prepared by dropping sodium alginate into solution of calcium chloride (3% w/w) under continuous agitation. Calcium alginate particles formed (mean diameter, 1083 μm) were washed and dried to be used in adsorption/ion exchange experiments [11].

Kinetic studies were carried out using single nitrate solutions of $Cu^{2+}$, $Cd^{2+}$, $Pb^{2+}$, and $Ni^{2+}$ of 3 mmol/L (Vetec, Brazil) and a bicomponent equimolar solution of $Cu^{2+}$and $Cd^{2+}$ (1 mmol/L for each metal). Values of pH were corrected using $NH_4OH$ and $HNO_3$.

All runs were conducted in finite baths at 25°C using 1 g of alginate immersed in 0.1 L of metallic solutions. Samples of these solutions were taken at different running times, and after filtration, the concentration of solutions was analyzed through atomic absorption spectrophotometry.

Mathematical modeling of the ion diffusion process in ion exchanger provided relevant information on mass transfer that is essential to the ion exchange/adsorption system design. The diffusion process in a solid matrix was described for the second Fick's law. In the spherical coordinate system, the concentration gradients are negligible in the angular direction, and the second Fick's law is represented by Eq. (3):

$$\frac{\partial q}{\partial t} = D_e \frac{1}{r} \frac{\partial}{\partial} \left( r \frac{\partial q}{\partial r} \right) \tag{3}$$

where $q$ is the ion capacity in ion exchanger (mg/g), $D_e$ is the ion diffusion coefficient in the adsorbent/ion exchanger ($cm^2/s$), $t$ is time (s), and $r$ is the radial direction (cm).

In this modeling, it was considered that the adsorbent was initially free of metal, the ion diffusivity was constant, the concentration in the fluid phase was homogeneous, and external resistance in the liquid film was negligible due to the agitation. The initial and boundary conditions used are described by Eqs. (4)–(6):

$$\text{at } t = 0 : q = q_0 \tag{4}$$

$$\text{at } r = R \text{ and } t > 0 : q = 0 \tag{5}$$

http://dx.doi.org/10.5772/60864

$$\text{at } r = 0 \frac{\partial q}{\partial r} = 0 \tag{6}$$

The average concentration of the metal ion exchanger is given by Eq. (7):

$$\frac{\bar{q}(t) - q_{eq}}{q_0 - q_{eq}} = 6\sum_{j=1}^{\infty}\left(\frac{1}{\gamma_j^2} e^{-\gamma_j Fo_M}\right) \tag{7}$$

where

$$Fo_{_M} = \frac{D_{ef} t}{R^2}; \gamma_j = j\pi$$

where $\gamma$ is the $j$ component of the activity coefficient, $D_{ef}$ is the effective diffusivity ($m^2/s$), and $R$ is the radius of the particle (m).

The metal concentration in the fluid phase is obtained from an overall mass transfer balance, represented by Eq. (8):

$$C(t) = \left(C_0 V - m_s \bar{q}(t)\right) / V \tag{8}$$

where $C_0$ is the initial concentration of metal in the fluid phase (mg/L), $\bar{q}$ is the metal incoming average capacity in the adsorbent ($mg_{metal}/g_{alginate}$), $m_s$ is the mass of bioadsorbent/ion exchanger (g dry basis), and $V$ is the volume of the solution ($dm^3$).

The method "golden search" was used to determine the effective diffusion coefficient of ions in bioadsorbent/ion exchanger to minimize the objective function given by Eq. (9):

$$F_{obj} = \sum_{j=1}^{n}\left(C_j^{MOD} - C_j^{EXP}\right)^2 \tag{9}$$

where $n$ is the number of experimental data, $C_j^{EXP}$ is the ion concentration in solution determined experimentally (mEq/L), and $C_j^{MOD}$: ion concentration in the solution calculated by the model (mg)

Figure 3 shows experimental results of the kinetics of the process and results obtained with the mathematical modeling for different metals in this study. The metal ions nickel, lead, and copper showed adsorption and desorption, indicating the competitiveness of metal ions (with calcium present in alginate) by the occupation of the active sites. The model used does not

consider this competitiveness, but only the adsorption of the ions of interest, resulting in slightly different values when compared to the experimental data.

Table 1 shows the quantities of metal ions removed from the single solutions by adsorption/ion exchange process. It appears that nickel was less adsorbed (0.92 mmol Ni/$g_{calcium\ alginate}$) in equilibrium. Indeed, alginic acid has a greater affinity for calcium than for nickel [12]. In a study of removal of different metals using calcium alginate, it was obtained the following amounts adsorbed: 0.247 mmol Cu/g, 0.138 mmol Cd/g, and 0.247 mmol Pb/g [13]. Although the conditions used were different from those used in this work, it can be seen that the alginate showed the same order of adsorptive capacity, or $Cu^{2+} > Pb^{2+} > Cd^{2+}$; in the case of this study (Table 1), it was $Cu^{2+} > Pb^{2+} > Cd^{2+} > Ni^{2+}$.

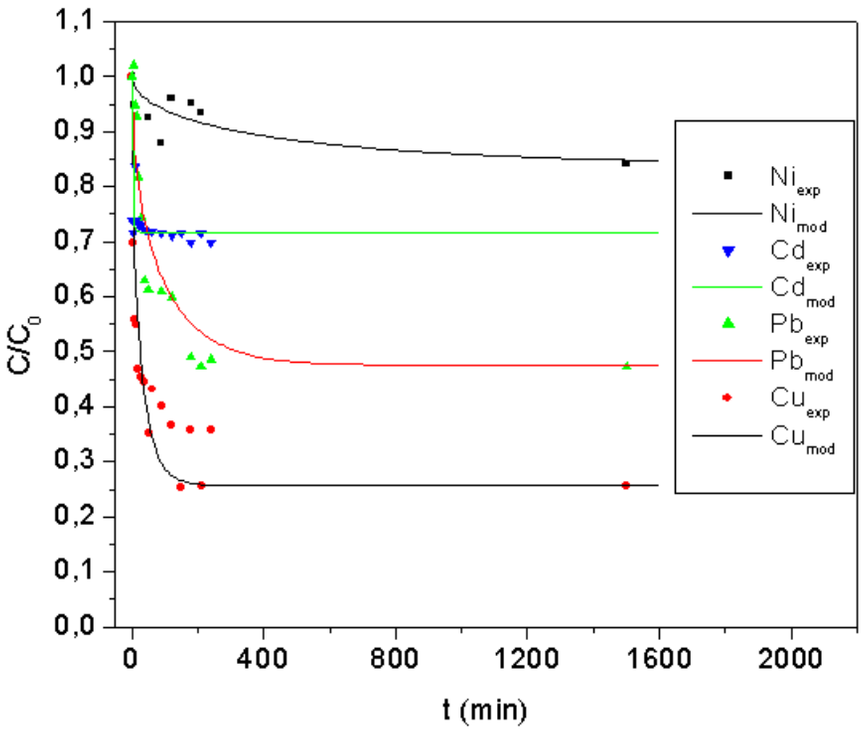


**Figure 3.** kinetic curves for different metal ions in monocomponent solutions for the adsorption/ion exchange into calcium alginate particles.

| Copper | Cadmium | Nickel | Lead |
|---|---|---|---|
| 4.658 | 1.792 | 0.987 | 3.106 |

**Table 1.** Adsorbed amount ($mmol_{metal}/g_{alginate}$) of different metals in the process of adsorption/ion exchange using single solutions.

The results obtained in finite bath for copper-cadmium binary mixture are shown in Figure 4. It is observed that copper was significantly more removed than cadmium. The adsorbed amount of copper and cadmium was 1.746 mmol Cu/$g_{calcium\ alginate}$ and 0.661 mmol Cd/$g_{calcium}$

http://dx.doi.org/10.5772/60864

$_{alginate}$, respectively. The greater affinity of calcium alginate to copper may be due to the chemical parameters listed in Table 2. The higher the electronegativity and the reduction potential and the lower the ionic radius, the easier the ion exchange/adsorption [14]. In this case, copper is more susceptible to ionic interaction with the alginate than cadmium because it presents all the favorable parameters to the ion exchange.

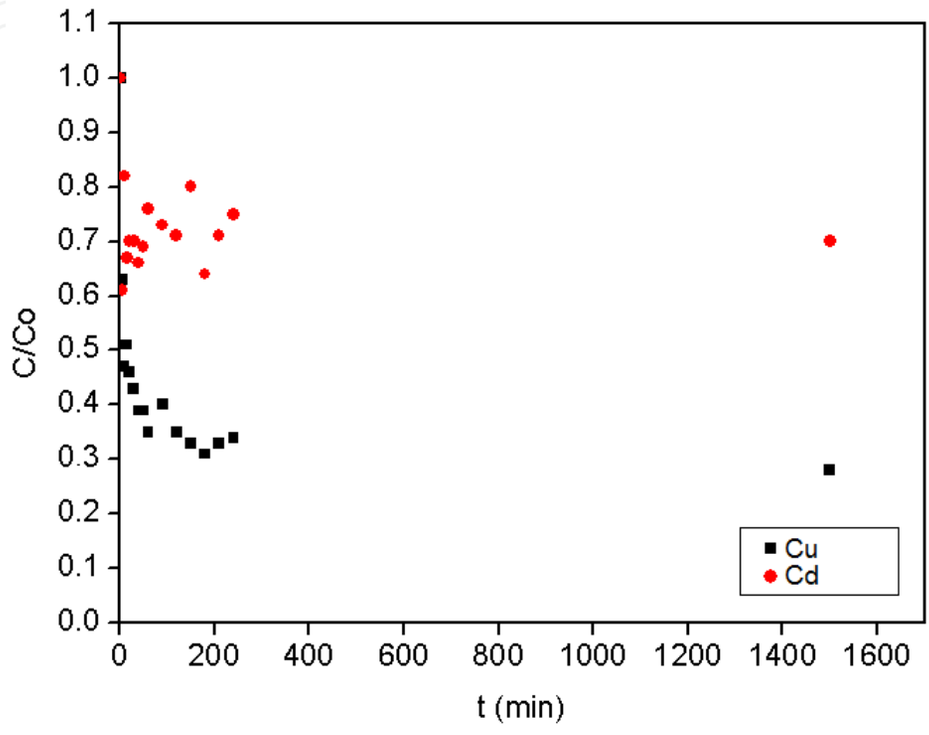


**Figure 4.** Kinetics of copper and cadmium in binary solution in the adsorption/ion exchange by calcium alginate particles.

| | Copper | Cadmium | Lead | Nickel | Calcium |
|---|---|---|---|---|---|
| **Atomic mass (g/mol)** | 63.546 | 112.411 | 207.200 | 58.710 | 40.080 |
| **Electronegativity** | 1.9 | 1.7 | 1.8 | 1.8 | 1.0 |
| **Ionic radius (Å)** | 0.73 | 0.97 | 0.132 | 0.69 | 0.99 |
| **Chemical reduction potential (V)** | 0.34 | –0.40 | –0.13 | –0.23 | –2.68 |

Source: reference [11].

**Table 2.** Chemical properties of divalent cations.

The diffusion capacity of the metal ions in the alginate particles analyzed was evaluated considering the Fick's law, and the respective values are shown in Table 3. It is observed that the cadmium showed higher diffusion capacity, and nickel is the metal resulting in an

increased resistance to intraparticle diffusion; thus, the metal adsorption order was $Cd^{2+}$ > $Cu^{2+}$ > $Pb^{2+}$ > $Ni^{2+}$. However, experimental results obtained with single and binary solutions were $Cu^{2+} > Pb^{2+} > Cd^{2+} > Ni^{2+}$ and $Cu^{2+} > Cd^{2+}$, respectively, indicating that this parameter cannot solely describe the metal affinity of alginate. Therefore, it becomes necessary to evaluate other properties of the ion exchanger/adsorbent.

| Metal | Diffusion capacity ($cm^2$/min) |
|---|---|
| Copper | 7.44E–06 |
| Cadmium | 8.38E–05 |
| Lead | 2.19E–06 |
| Nickel | 4.57E–07 |

**Table 3.** Diffusion capacity of metal ions in calcium alginate.

*4.1.2. Copper equilibrium study of calcium alginate particles in a static system*

The isotherm of Langmuir model (L) is widely used due to its simplicity and theoretical basis and is expressed by Eq. (10). The parameter $b$ is the ratio between the rate of adsorption and desorption and is directly related to Henry's constant. High values of $b$ indicate high affinity of the ions by the active sites of the material. The parameter $q_{max}$ indicates the total number of active sites available, and $q^*$ and $C^*$ represent the metal removal capacity at equilibrium in the solid and liquid phases, respectively. Adsorption is very favorable when values of $b.C^* >> 1$; however, if $b.C^* < 1$, the isotherm is almost linear.

$$q^* = \frac{q_{max} \cdot b \cdot C^*}{1 + b \cdot C^*} \tag{10}$$

The Freundlich isotherm is an empirical adjustment of a model, which considers that the energy of the active sites of the adsorbent material is heterogeneous and that the adsorption process is reversible. It corresponds to the exponential distribution heats of adsorption and is expressed by Eq. (11), where $k_d$ and $n$ are constants in the model. This model does not predict the saturation of the adsorbent, allowing an infinite number of layers covering the ionic adsorbent [15]. When $n < 1$, it is typically a liquid adsorption [16].

$$q^* = k_d \cdot C^{*n} \tag{11}$$

Figure 5 shows the equilibrium data in finite bath by contacting 1 g of hydrated alginate with 100 mL of metal solution with different initial concentrations [11]. The Langmuir isotherm model (Equation 10) and the Freundlich model (Equation 11) were fitted to the experimental equilibrium data as shown in Figure 5, and the respective values of model parameters are presented in Table 4.

http://dx.doi.org/10.5772/60864

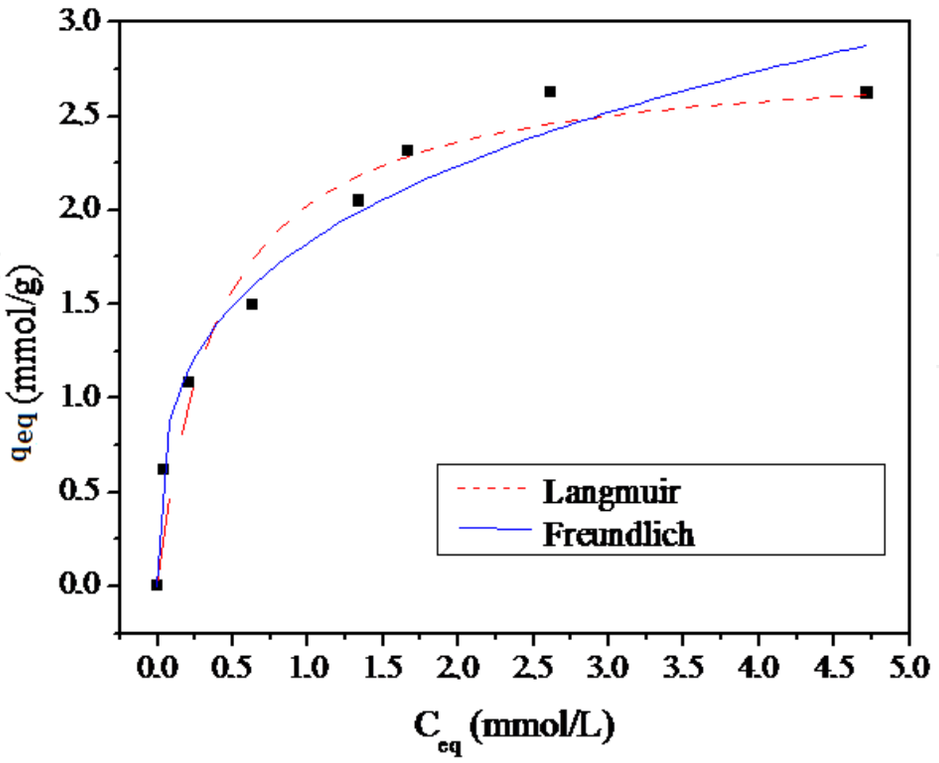


**Figure 5.** Cu adsorption isotherm in calcium alginate fitted by the Langmuir and Freundlich models.

| | | | |
|---|---|---|---|
| **Langmuir** | $q_{max}$ (mg/g) | $b$ (mg/L) | $R^2$ |
| | 2.8323 | 0.3977 | 0.9623 |
| **Freundlich** | $k_d$ | $n$ | $R^2$ |
| | 1.8269 | 0.2924 | 0.9739 |

**Table 4.** Parameters of Langmuir and Freundlich models.

According to Table 4, both models could satisfactorily adjust the equilibrium experimental data for copper ions. The isotherm obtained in Figure 5 can be classified as type I [17], which is characteristic of the Langmuir isotherm where adsorption occurs only in monolayer. Moreover, these models have also been adequately used to describe the process of removing metal ions using calcium alginate (Ca-Alginate) particles [18,19].

In the ion exchange process involving the binary system of copper and cadmium ions in calcium alginate (systems $Cu^{2+}$-$Ca^{2+}$, $Cd^{2+}$-$Ca^{2+}$, and $Cu^{2+}$-$Cd^{2+}$), it was considered only the presence of the higher affinity ion, or for the $Cu^{2+}$-$Ca^{2+}$ system, only the presence of $Cu^{2+}$ species, for $Cd^{2+}$-$Ca^{2+}$system, the presence of $Cd^{2+}$ species, and for the $Cu^{2+}$-$Cd^{2+}$ system, the presence of copper [11]. Many single adsorption isotherms were evaluated for the binary systems, as shown in Table 5 and in Figure 6.

| Model | Parameters | Equation |
|---|---|---|
| Langmuir | $q_{max}$, $b$ | $q^* = \frac{q_{max} \cdot b \cdot C^*}{1 + b \cdot C^*}$ |
| Freundlich | $q_{max}$, $n$ | $q^* = k_d \cdot C^{*n}$ |
| Redlich–Peterson | $q_{max}$, $b$, $n$ | $q^* = \frac{q_{max} b C^*}{1 + b C^{*n}}$ |
| Toth | $q_{max}$, $b$, $n$ | $q^* = \frac{q_{max} C^* b^{1/n}}{(1 + b C^{*n})^{1/n}}$ |
| Radke–Praunitz | $q_{max}$, $b$, $n$ | $q^* = \frac{q_{max} C^* b}{(1 + B C^*)^n}$ |
| Sips | $q_{max}$, $b$, $n$ | $q^* = \frac{q_{max} b C^{*n}}{1 + b C^{*n}}$ |

**Table 5.** Adsorption isotherm models used for the binary system by considering only the presence of the ion of higher affinity.

| Model | Parameters | $F_{obj}$ | $R^2$ |
|---|---|---|---|
| Langmuir | $q_{max}$ (mEq/g) = 14.540<br>b (L/mEq) = 0.139 | 0.069 | 0.990 |
| Freundlich | $K$ (mEq/g) = 2.020<br>$n$ = 0.658 | 1.054 | 0.982 |
| Redlich–Peterson | $q_{max}$(mEq/g) = 20.7841<br>b(L/mEq) = 0.091<br>$n$ = 1.1331 | 0.56198 | 0.991 |
| Toth | $q_{max}$(mEq/g) = 13.207<br>b(L/mEq) = 0.108<br>$n$ = 1.1455 | 0.566 | 0.990 |
| Radke–Prausnitz | $q_{max}$(mEq/g) = 40.555<br>b(L/mEq) = 4.677<br>$n$ = 2.139 | 0.549 | 0.991 |
| Sips | $q_{max}$(mEq/g) = 25.332<br>b(L/mEq) = 0.077<br>$n$ = 0.847 | 0.592 | 0.988 |

**Table 6.** Parameters obtained for the single component isotherm models for the system $Cu^{2+}$–$Ca^{2+}$.

All models resulted in satisfactory determining coefficient values ($R^2$), indicating proper fit to the experimental data (Table 6).

http://dx.doi.org/10.5772/60864

The Sips model was successfully used to represent the removal of copper and cadmium ions in Ca-Alginate particles, mainly when compared to Langmuir and Freundlich models [19]. It happened due to the heterogeneity of the surface of the adsorbent, especially for metals of lower-affinity with the alginate.

Although in the system involving the $Cd^{2+}$-$Ca^{2+}$ ions, experimental data have been acceptable adjusted, the interference of calcium on $Cd^{2+}$-$Ca^{2+}$ system was higher when compared to $Cu^{2+}$-$Ca^{2+}$system, indicating that the alginate had a higher affinity for copper than for cadmium [11,20].

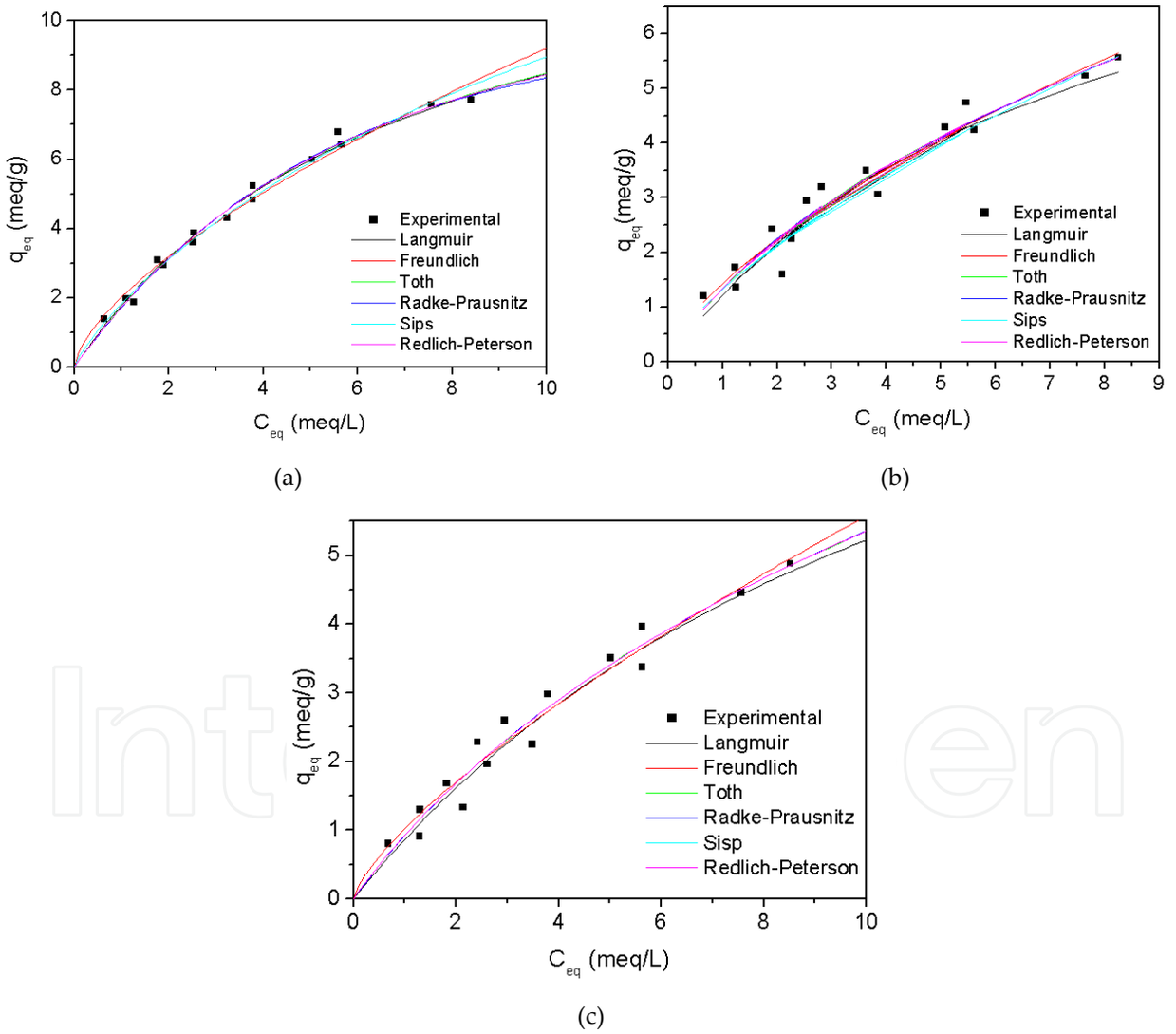


**Figure 6.** $Cu^{2+}$ adsorption isotherms for Ca-Alginate system (a), Cd-Alginate system (b), and $Cd^{2+}$ adsorption isotherms for Ca-Alginate system (c) in monocomponent system [11,20].

*4.1.3. Copper removal in dynamic system: adsorption and desorption cycles*

The study of removing copper ions in the calcium alginate particles porous bed column was assessed through adsorption and desorption cycles. The experiments were performed in a glass column (internal diameter, 1.4 cm) filled with 9.80 g of calcium alginate particles to reach a bed height of 13.3 cm. Flow tests were performed with 3 mL/min for adsorption and desorption cycles. The initial concentration of copper used in the adsorption step was 4.72 mmol/L. In the desorption step, calcium chloride solution with a concentration of 18 mmol/L was employed as eluent. The amount of copper removed in the column experiment was calculated by the Eq. (12). The experimental conditions were defined from fluid dynamic preliminary studies.

$$Q = \frac{C_0 F}{1000m} \cdot \int_0^t \left( \frac{C_0 - C}{C_0} \right) \cdot dt \tag{12}$$

where $C_0$ is the initial concentration of metal (mmol/L), $C(t)$ is the metal concentration at time $t$ (mmol/L), $F$ is the volumetric flow of the solution (mL/min), $m$ is the mass of alginate (g), $Q$ is the metal removal capacity at time $t$ ($mg_{metal}/g_{bioadsorvente}$), and $t$ is time (min).

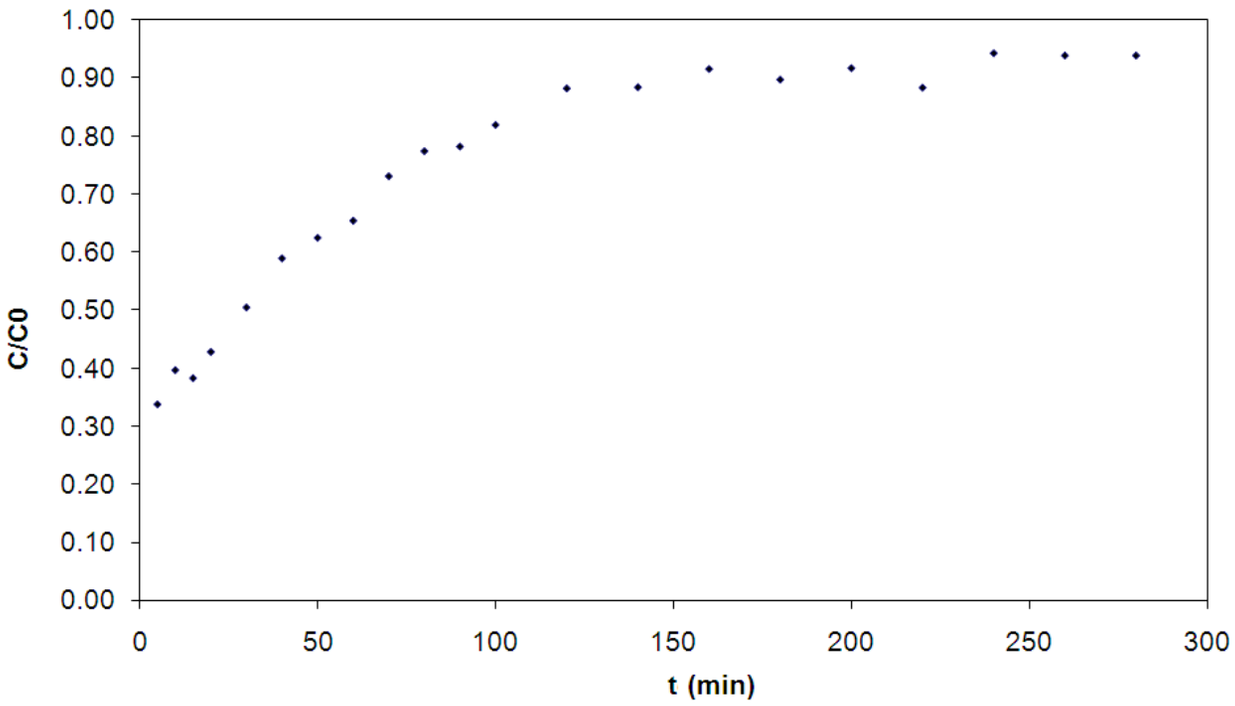


**Figure 7.** Kinetics of adsorption of copper ions in porous bed (Initial copper concentration 4.72 mmol/L).

Aliquots were withdrawn periodically, and the pH of feed metallic solution was monitored throughout the process, which was maintained between 4 and 4.5. The copper removal kinetics is shown in Figure 7. From the breakthrough curve, the complete saturation of the

bed was reached at 140 min of process. The total amount of copper removed given by Eq. (12) was 2.83 mmol/g.

Copper was desorbed from alginate employing calcium chloride solution with a concentration of 18 mmol/L. Initially, it is known that alginate has a greater affinity for copper than the alginate. However, when alginate is saturated with copper ions and comes into contact with a solution containing a high concentration of calcium, copper alginate may desorb ions and adsorb calcium ions to achieve chemical equilibrium. However, in this case, which the ions being adsorbed has a lower affinity, the process occurs only when calcium is present in solution at high concentrations. The kinetics of this process step is in Figure 8. The flow rate used, as well as in adsorption cycle, was 3 mL/min. The calcium alginate recovery was 97%. The equilibrium time of the desorption system was close to 150 min.

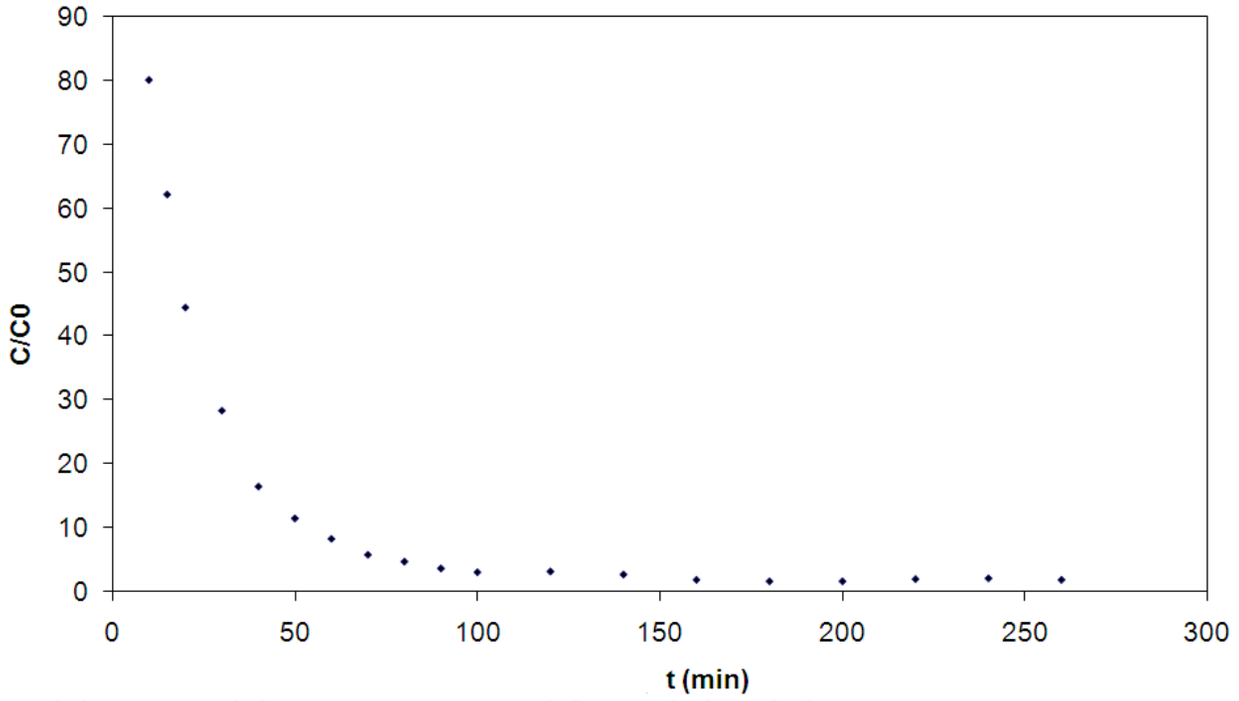


**Figure 8.** Kinetics of copper desorption in bed of porous calcium alginate particles.

### 4.2. Case study 2: Equilibrium and dynamic studies of $Mn^{2+}$ and $Cr^{3+}$ in bone char

It is already known that metal ions, like manganese and chromium, when present in wastewaters may contaminate the environment if not adequate treated. In particular, high concentrations of manganese ion in water promote corrosion of pipes, and as this metal is toxic to the brain, it may cause neurological disorders. The hexavalent chromium ion is another highly toxic metal present in wastewater, which is related to cancer diseases. The trivalent chromium specie is less toxic than the hexavalent one, and it can be easily oxidized in wastewater treatment through reduction of manganese ions. The removal of these metals from wastewater can be carried out by adsorption/ion exchange processes using bone char [21].

Bone char is an untypical kind of activated carbon due to its animal origin. It is composed by around 10% carbon and 90% calcium phosphate. Figure 9 illustrates the bone char structure. The calcium phosphate in bone char is present as hydroxyapatite—$Ca_{10}(PO_4)_6(OH)_2$ [22] with a calcium-to-phosphate ratio of 1.67, and unit cell dimensions of $a = b = 9.432$ Å and $c = 6.881$ Å [23].

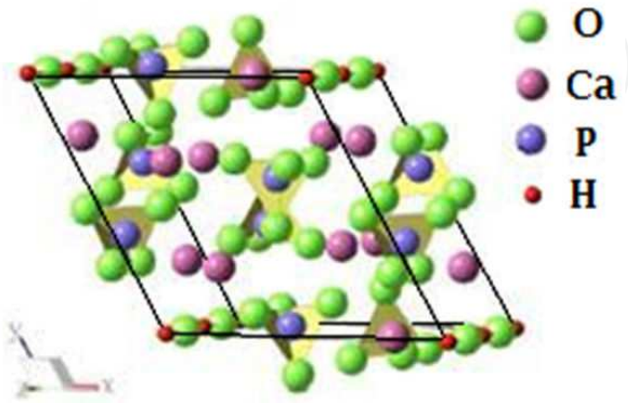


**Figure 9.** The hydroxyapatite structure viewed along the *c*-axis. The yellow polyhedrons represent the phosphate groups [23].

Cation exchange in bone char may occur preferentially with calcium ions, depending on radius and electronegativity of the incoming ion [24]. Under this consideration, bone char can be quite useful material to be used for removal of both $Mn^{2+}$ and $Cr^{3+}$ through calcium ion exchange.

*4.2.1. Materials*

The bovine bone char was crushed, sieved (20–28 mesh Tyler, average particle diameter of 0.725 mm), and elutriated with abundant water to remove fine particles and finally dried at 80°C for 24 h. The exchanger particulate material was characterized through $N_2$ adsorption, scanning electron microscopy (SEM), and infrared spectrophotometry (FTIR). Zero point charge (ZPC) was obtained based on references [25, 26].

Solutions of 15 mEq/L of $CrCl_3.6H_2O$ and $MnCl_2.4H_2O$ were used in single metal removal. Binary solutions containing 7.5 mEq/L of each cation were also used.

*4.2.2. Results and discussion*

$N_2$ isotherm showed that the bone char was predominantly mesoporous material with hysteresis and a BET area of 100 $m^2$/ g, which is a typical for this kind of solid material (Figure 10).

Scanning electron microscopy (SEM) of the bone char sample (Figure 11) presented heterogeneity morphology of particles and channels similar to results already reported [27].

FTIR spectrum presented in Figure 12 depicts a characteristic band at 1380 $cm^{-1}$ attributed to $^{\nu}NO_3$ group, bands at 3450 $cm^{-1}$, 603 $cm^{-1}$ due to –OH group vibration, band at 1640 $cm^{-1}$ due

http://dx.doi.org/10.5772/60864

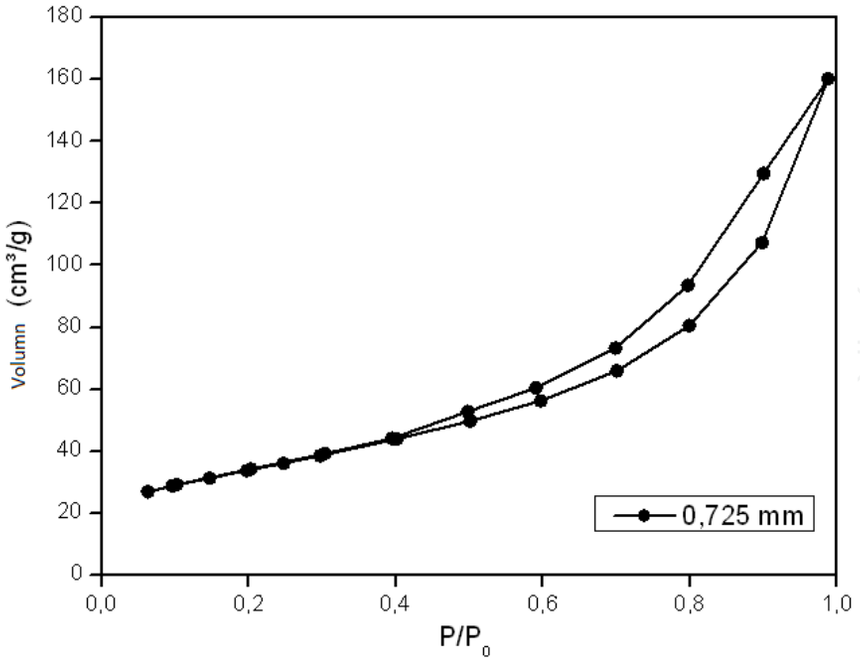


**Figure 10.** Nitrogen adsorption–desorption isotherm at 77K of bone char.

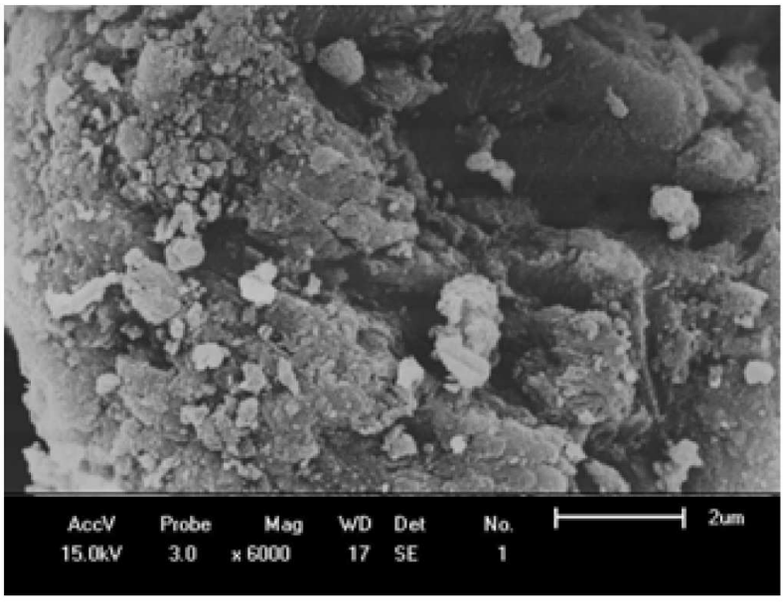


**Figure 11.** Micrograph obtained by SEM of the bone char.

to $CO_3^{2-}$, and a band at 1038 $cm^{-1}$ attributed to the molecular vibration of $PO_4^{3-}$ [22]. The balancing cations of such groups may be exchanged when in contact with electrolyte solutions.

The superficial zero point charge (ZPC) was pH 7.9. As the pH values solutions was 5–6, the surface charge was predominated by positively charged $\equiv CaOH_2^+$ and neutral $\equiv POH^0$ sites. The surface charge was then positive [28].

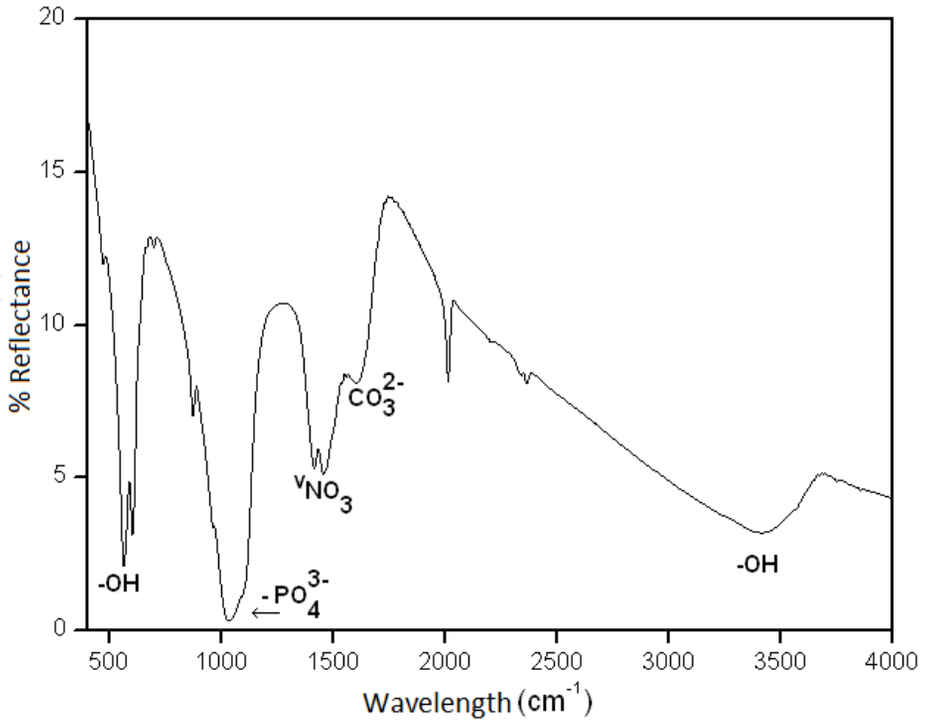


**Figure 12.** FTIR Spectrum of the bone char samples.

Single and bicomponent isotherms were obtained at 25°C, 30°C, and 40°C. Although bone char is a typical ion exchanger, ions may be also retained by adsorption mechanism. Actually, it is difficult to find out an equation that presents, mathematically, the contribution of all phenomena involved. Classical adsorption equations such as the Langmuir, Freundlich, and Langmuir–Freundlich models are commonly used [2].

Single isotherms are shown in Figure 13. Chromium isotherms are more favorable than the manganese ones. This can be seen through the steeper shape and higher amounts of ion retained, which is a consequence of higher ion charge and electronegativity [24].

Temperature seemed to have a higher influence in chromium removal when temperature was increased to 40°C. Probably, a reduction of the hydration radius occurred exposing the electronegativity and promoting the exchange process. According to the amount retained observed qualitatively in all temperatures, the selectivity order is $Cr^{3+} > Mn^{2+}$.

$Cr^{3+}$ and $Mn^{2+}$ ions may be located in site II, at the edge of the hydroxide channel of the hydroxyapatite. In site II, there would be a shift of the ion. In site I, $Cr^{3+}$ and $Mn^{2+}$ ions would be compressed within the local cluster.

The ion exchange process may be expressed as follows [24]:

$$CaHOAP + Mn^{2+} = MnHOAP + Ca^{2+}$$

$$3CaHOAP + 2Cr^{3+} = Cr_2\left(HOAP\right)_3 + 3Ca^{2+}$$

http://dx.doi.org/10.5772/60864

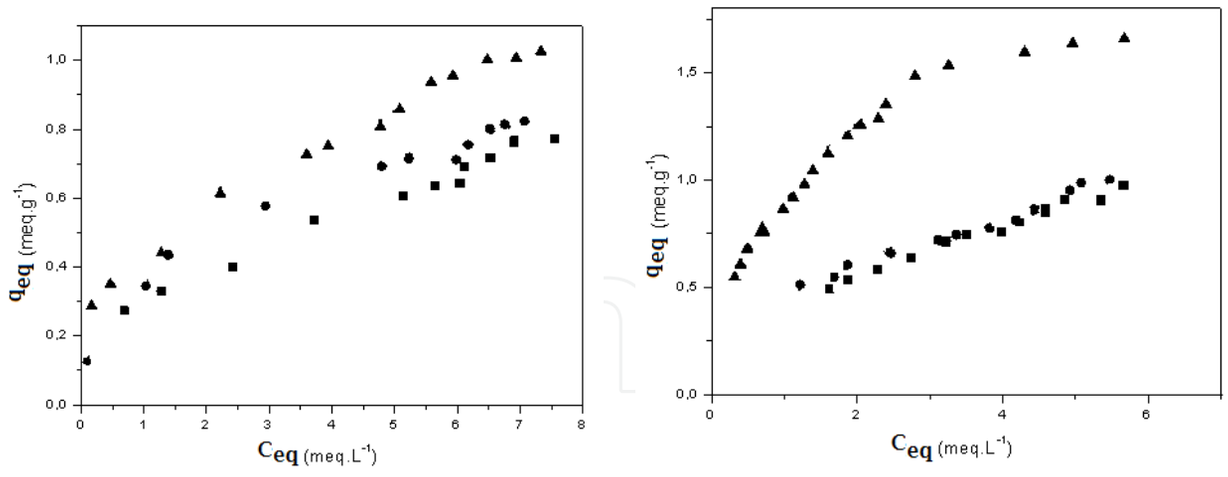


**Figure 13.** (a) $Mn^{2+}$ isotherms; (b) $Cr^{3+}$ isotherms. (■)25°C, (▲) 30°C, (●) 40°C.

Due to pH < ZPC, replacements below may also happen:

$$\equiv POH^0 + Mn^{2+} = \equiv POMn^+ + H^+$$
$$\equiv POH^0 + Cr^{+3} = \equiv POCr^{+2} + H^+$$

Moreover, besides the ion exchange, the multilayer adsorption may occur as the typical plateau of ion exchange monolayer is not seen in the isotherms. In agreement with such phenomena, experimental data may be better represented by the Langmuir–Freundlich isotherms [29]. Tables 7 and 8 show such results.

| Parameter | 25°C | 30°C | 40°C |
|---|---|---|---|
| | | **Langmuir** | |
| $q_{max}$ | 0.885 ± 0.073 | 0.986 ± 0.036 | 0.962 ± 0.076 |
| $B$ | 0.495 ± 0.136 | 0.539 ± 0.066 | 1.258 ± 0.523 |
| $R^2$ | 0.9136 | 0.9787 | 0.8199 |
| | Freundlich | | |
| $k_f$ | 0.301 ± 0.017 | 0.342 ± 0.013 | 0.472 ± 0.023 |
| $N$ | 0.446 ± 0.033 | 0.446 ± 0.023 | 0.367 ± 0.029 |
| $R^2$ | 0.9736 | 0.986 | 0.9698 |
| | Langmuir–Freundlich | | |
| $q_{max}$ | 1.341 ± 0.573 | 1.435 ± 0.395 | 1.796 ± 0.687 |
| $B$ | 0.279 ± 0.144 | 0.321 ± 0.112 | 0.281 ± 0.138 |
| $1/n$ | 0.643 ± 0.159 | 0.714 ± 0.141 | 0.700 ± 0.134 |
| $R^2$ | 0.996 | 0.993 | 0.995 |

**Table 7.** Equilibrium parameters for manganese ions.

| Parameter | 25°C | 30°C | 40°C |
|---|---|---|---|
| | **Langmuir** | | |
| $q_{max}$ | 1.507 ± 0.082 | 1.305 ± 0.097 | 1.836 ± 0.066 |
| $B$ | 0.287 ± 0.033 | 0.450 ± 0.087 | 1.090 ± 0.121 |
| $R^2$ | 0.9772 | 0.9217 | 0.9612 |
| | Freundlich | | |
| $k_f$ | 0.381 ± 0.011 | 0.444 ± 0.019 | 0.897 ± 0.020 |
| $N$ | 0.531 ± 0.020 | 0.452 ± 0.031 | 0.408 ± 0.019 |
| $R^2$ | 0.9886 | 0.9627 | 0.9678 |
| | Langmuir–Freundlich | | |
| $q_{max}$ | 1.792 ± 0.216 | 1.263 ± 0.589 | 3.789 ± 0.013 |
| $B$ | 0.261 ± 0.036 | 0.503 ± 0.029 | 0.318 ± 0.145 |
| $1/n$ | 0.779 ± 0.052 | 0.871 ± 0.049 | 0.571 ± 0.091 |
| $R^2$ | 0.987 | 0.989 | 0.983 |

**Table 8.** Equilibrium parameters for chromium ions.

The binary isotherms are shown in Figure 14. As expected, chromium is again more retained, although the shape of the isotherms is completely different. This is a consequence of competition of both ions for site II.

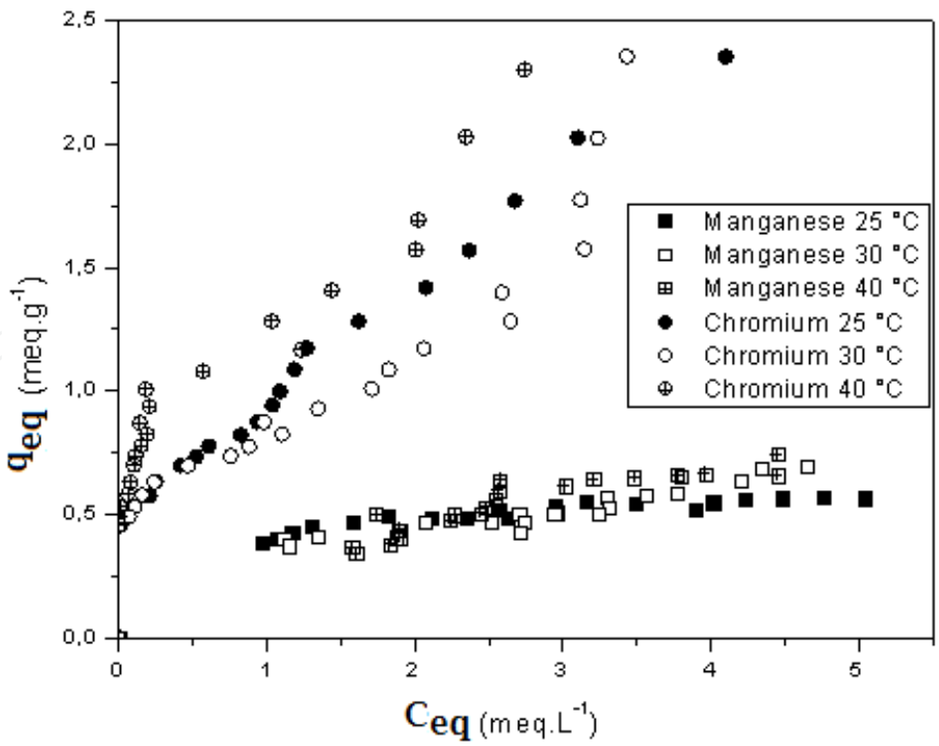


**Figure 14.** Isotherms for $Mn^{2+}/Cr^{3+}$ binary system in bone char.

Again, the Langmuir–Freundlich model was the one that best represents bicomponent exchange in bone char sample, as seen in Table 9 with the lowest objective function. The parameter $b_i$ for the bicomponent adjustment for the Langmuir–Freundlich model is lower than the ones estimated for the single isotherms due to the competition to site II. Nevertheless, $q_{max}$ are much higher than the single values, indicating a physisorption process where more ions are retained with weaker energy.

| Parameters | 25°C | 30°C | 40°C |
|---|---|---|---|
| | Extended Langmuir [30] | | |
| $b_1$ (L/mEq) | 2.597 | 0.993 | 3.000 |
| $b_2$ (L/mEq) | 0.925 | 0.102 | 0.007 |
| $q_{m1}$ (mEq/g) | 2.914 | 2.097 | 2.184 |
| $q_{m2}$ (mEq/g) | 0.967 | 4.121 | 39.644 |
| Objective function | 1.880 | 1.550 | 4.287 |
| | Jain and Snowyink [31] | | |
| $b_1$ (L/mEq) | 130.1 | 11.542 | 16.16 |
| $b_2$ (L/mEq) | 71.19 | 0.211 | 0.047 |
| $q_{m1}$ (mEq/g) | 1.222 | 1.015 | 1.303 |
| $q_{m2}$ (mEq/g) | 0.606 | 2.304 | 5.565 |
| Objective function | 1.183 | 0.317 | 1.658 |
| | Langmuir–Freundlich | | |
| $b_1$ (L/mEq) | 0.296 | 0.178 | 0.251 |
| $b_2$ (L/mEq) | 0.394 | 0.053 | 0.026 |
| $n_1$ | 0.260 | 0.297 | 0.203 |
| $n_2$ | 0.370 | 0.550 | 0.828 |
| $q_{m1}$ (mEq/g) | 5.775 | 6.324 | 6.045 |
| $q_{m2}$ (mEq/g) | 1.592 | 7.192 | 10.931 |
| Objective function | 0.241 | 0.148 | 0.374 |

$Cr^{3+}$ = subscript 1; $Mn^{2+}$ = subscript 2.

**Table 9.** Model parameters for $Mn^{2+}/Cr^{3+}$ binary system.

### 4.3. Case study 3: Dynamic ion exchange in multicomponent solution

Zeolites NaY and NaX are well-known ion exchangers. In this study, these zeolites were used for chromium uptake from bicomponent solutions. As it will be seen, multicomponent ion

exchange in dynamic systems may provide some overshooting ($C/C_o > 1$) related to a sequential ion exchange, where a more preferable cation with lower diffusion will be exchanged not by the balancing ion but by the competing ion previously retained [32].

*4.3.1. Materials and methods*

NaY has the unit cell composition of $Na_{51}(AlO_2)_{51}(SiO_2)_{141}$ on a dry basis, and a cation exchange capacity (CEC) of 3.90 mEq/g NaX zeolite has a unit cell composition of $Na_{81}(AlO_2)_{81}(SiO_2)_{111}$, which corresponds to a higher cation exchange capacity of 5.96 mEq/g.

First, the zeolite samples were added to 1 mol/L solution of NaCl four times at 60°C under stirring. Samples were then washed at the end of each addition with 2 L of hot deionized water and finally oven-dried at 100°C. Such procedure aimed to originate a homoionic sodium zeolite. Samples were pelletized (average diameter size of 0.180 mm).

Reagent-grade $CrCl_3$ $9H_2O$, $MgCl_2$ $6H_2O$, $CaCl_2$ $2H_2O$, and KCl were used to obtain binary solutions, always containing chromium and another cation in an equivalent ratio of 1:1. The concentration of chromium solution was 18 mg/L.

The dynamic runs were conducted in a packed bed of a clear glass tube 0.9 cm ID and 30 cm long. The zeolite pellets were located in the middle of the column that operated isothermally at 30°C. The packed bed was composed of 1.60 g of NaY or 1.04 g of NaX in order to provide the same cation exchange capacity, whereas the system was fed at 9 mL $min^{-1}$ of ion solution. Although the packed bed heights were different for NaY and NaX zeolites, experiments conducted with the same cation exchange capacity will generate results to compare the performance of the zeolites, mainly when uptake efficiency is aimed.

*4.3.2. Results of the dynamic binary runs*

Breakthrough curves of metals ions in packed beds of NaY and NaX zeolites are presented in Figures 15 to 17. In all cases, except for the Cr/Mg system in NaX zeolite, some overshooting could be seen as $C/C_o$ reached values higher than 1. In such cases, the incoming ions were first uptaken. As their hydrated radii are smaller than the one for chromium, their diffusion into the zeolitic channels were improved. Rapidly, the incoming ions were exchanged. Chromium ions are much more preferred due to the trivalent charge, and after reaching the exchanging sites, they could replace the ion previously retained.

Besides the sequential ion exchange, it is also important to emphasize the influence of the ion exchanger. NaY and NaX zeolites are isomorph materials, and the only difference between them is the charge density in the packed bed. Denser sites of NaX may promote higher attraction with electrostatic instability due to repulsion of ions closely attracted. As a consequence, the ratio of chromium uptake up to its breakpoint time (tb)/cation exchange capacity (CEC) is less retained than in NaY system, as it can be seen in Table 10.

http://dx.doi.org/10.5772/60864

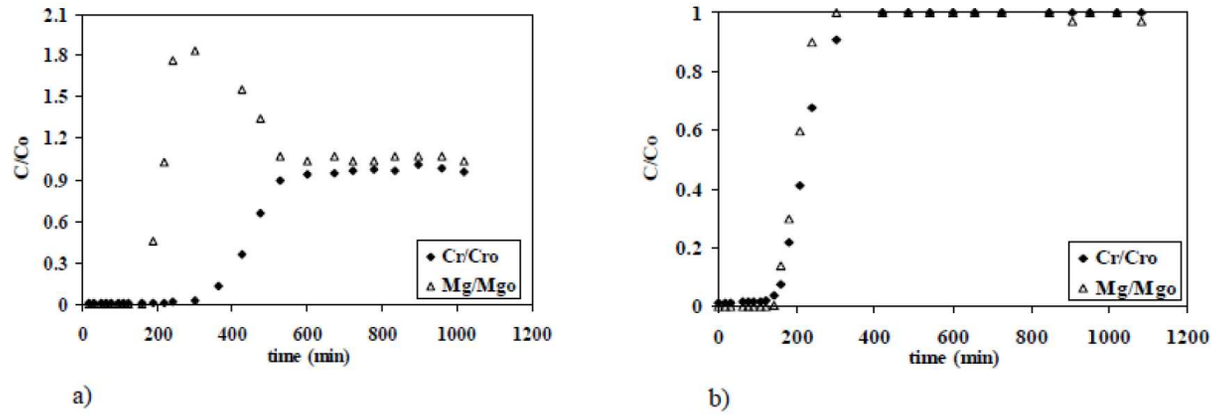


**Figure 15.** Breakthrough curves for the Cr-Mg competitive system: (a) NaY and (b) NaX.

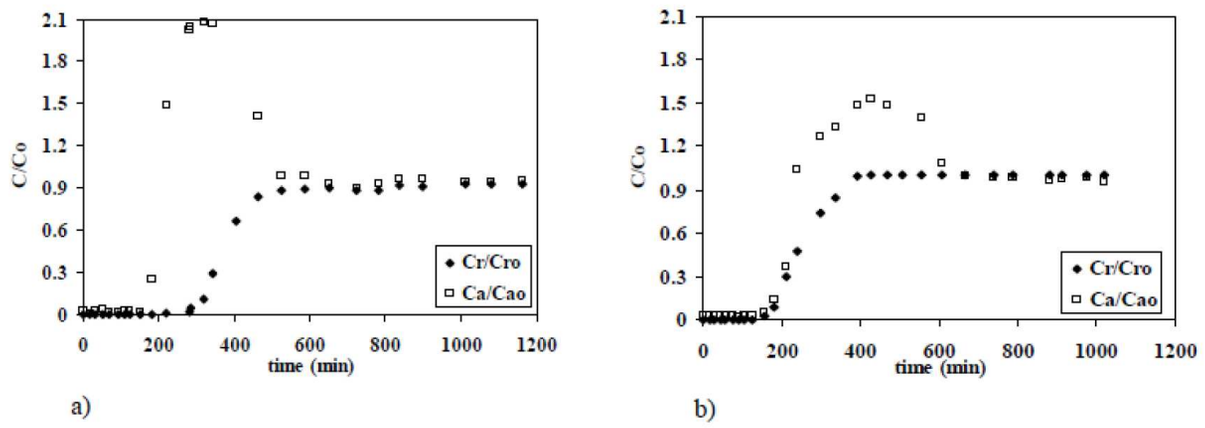


**Figure 16.** Breakthrough curves for the Cr-Ca competitive system: (a) NaY and (b) NaX.

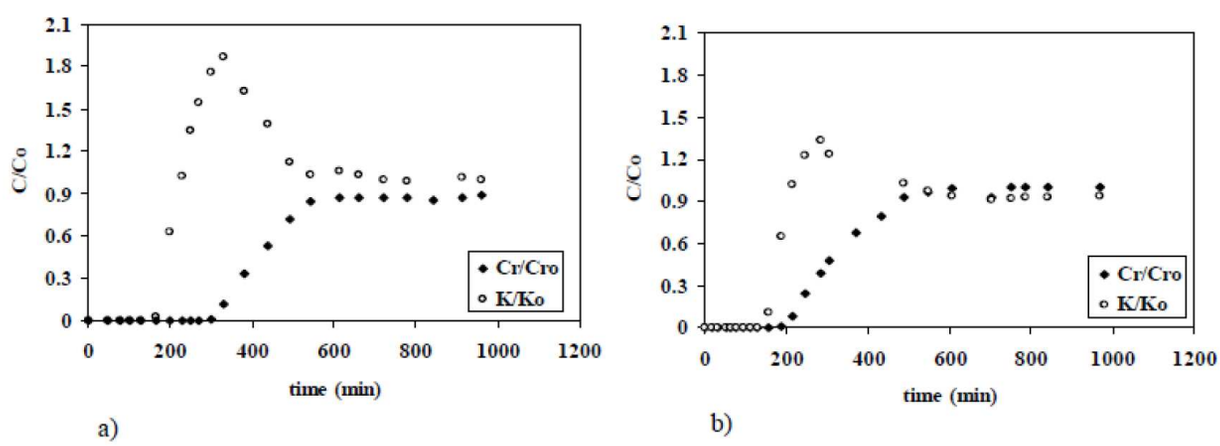


**Figure 17.** Breakthrough curves for the Cr-K competitive system: (a) NaY and (b) NaX.

| System | $U_{tb}^{Cr}/CEC$ | System | $U_{tb}^{Cr}/CEC$ |
|---|---|---|---|
| Cr-NaY | 0.69 | Cr-NaX | 0.71 |
| Cr/Mg-NaY | 0.54 | Cr/Mg-NaX | 0.27 |
| Cr/Ca-NaY | 0.51 | Cr/Ca-NaX | 0.31 |
| Cr/K-NaY | 0.66 | Cr/K-NaX | 0.41 |

$U_{tb}^{Cr}/CEC$= ratio of chromium uptake up to chromium breakpoint time (tb) and the cation exchange capacity of the column.

**Table 10.** Amount of chromium ions retained up to the breakpoint of 5% of the feed concentration.

## 5. General conclusions

Ion exchange is a much more complex phenomenon than adsorption as many ion exchangers may also act as adsorbents, increasing the difficulty in understanding the sorption removal.

Moreover, electrolytes add complexity in fluid phase and also in the solid phase. Ion charges and hydration energy of the incoming ions as well as charge density of the ion exchanger are undoubtedly factors that deserve detailed investigation, mainly for scaling-up proposals.

## Author details

Maria Angélica Simões Dornellas de Barros[1], Marcelino Luiz Gimenes[1], Melissa Gurgel Adeodato Vieira[2] and Meuris Gurgel Carlos da Silva[2]

1 Chemical Engineering Department, State University of Maringá, Maringá, PR, Brazil

2 School of Chemical Engineering, University of Campinas, Campinas, SP, Brazil

## References

[1] Helferich, F., Ion Exchange, EUA, Dover Publications Inc., 1995.

[2] Zagorodni, A.A., Ion Exchange Materials Properties and Applications, Great Britain, Elsevier, 2007.

[3] Febrianto, J., Kosasih, A., N., Sunarco, J., Ju, Y-H., Indraswati, N., Ismadji, S., J. Hazard. Mater., 2009, 162, 2–3, 616.

[4] Qui, H., Lu, L., Pan, B., Zhang, Q., Zhang, W., Zhang, Q., J. Zhejiang Univ. Sci. A, 2009,10, 715.

[5] Tseng, J., Chang, C., Chang, C., Chenc, Y., Chang, C., Ji, D., Chiud, C., Chiang, P., J. Hazard. Mat., 2009, 171, 370.

[6] Breck, D. W., Zeolite Molecular Sieves—Structure, Chemistry and Uses, Robert E. Kriger Publishing Co., USA, 1974.

[7] Barrer, R.M., Bull. Soc. Fr. Minéral. Cristallogr., 1974, 97, 89.

[8] Barros, M. Arroyo, P.A., Silva, E.A., Chap. 14. General aspects of aqueous sorption process in fixed beds, In: Mass Transfer—Advances in Sustainable Energy and Environment Oriented Numerical Modeling, InTech, Croatia, 2013, 361–386.

[9] Ostroski, I. C., Dantas, J. H., Silva, E. A., Arroyo, P. A., Barros, M. A. S. D., Adsoption Sci. Tech., 2012, 30, 4, 275.

[10] Ostroski, I.C., Silva, E.A., Arroyo, P.A., Barros, M.A.S.D., Fluid Phase Equilib., 2014, 372, 76.

[11] Welter, R. A., Estudo do equilíbrio dos sistemas binários e ternário de troca iônica dos íons cobre, cádmio e cálcio pelo biopolímero alginato. Campinas: Universidade Estadual de Campinas, UNICAMP, 2009. 197p. D.Sc. Thesis (in Portuguese).

[12] Davis, T. A., Volesky, B. Mucci, A. Wat. Res., 2003, 37, 4311.

[13] Huang, C., Cheng, Y.C., Liou, M. R., J. Hazard. Mater.,1996, 45, 265.

[14] Sag, Y., Kaya, A., Kutsal, T., Hydrometallurgy, 1998, 50, 297.

[15] Reed, B. E., Matsumoto, M. R., Sep. Sci. Technol., 1993, 28, 13, 2179.

[16] Ciola, R., Fundamentos da Catálise, Ed. Moderna, São Paulo, 1981. Davis, T. A., Volesky, B. Mucci, A., Water Res., 2003, 37, 4311.

[17] Brunauer, S., Deming, L.S., Deming, W. E., Teller, E., Bureau of Agricultural Chemistry and Engineering and George Washington University, 1940, 1723–1732.

[18] Lai, Y.L., Annaduarai, G., Huang, F.C., Lee, J.F., Bioresource Tech., 2008, 99, 6480.

[19] Papageorgiou, S. K., Kouvelos, F. K., Katsaros, F. K., Desalination, 2008, 224, 293.

[20] Vieira, M. G. A., Silva, M. G. C. Adsorção/Bioadsorção de Metais Pesados, Compostos Orgânicos e Corantes em Solução Aquosa In: Aplicações tecnológicas em sistemas particulados. 1 ed.São Carlos: ANIMERIS, 2011, 171–212 (in Portuguese).

[21] Oliveira, C. M., Remoção de Metais Pesados Utilizando Carvão Ativado. Maringá: Universidade Estadual de Maringá, UEM, 2012. 120p. MSc thesis (in Portuguese).

[22] Hassan, S. S. M., Awwad, N. S., Aboterika, A. H. A., J. Hazard. Mater. 2008, 154, 992.

[23] Snyders, R., Music, D., Sigumonrong, D., Schelnberger, B., Jensen, J., Schneider, J. M., Appl. Phys. Letters, 2007, 90, 193902.

[24] Takeuchi, Y., Arai, H. J., Chem. Eng. Jpn., 1990, 23, 75.

[25] Park, J., Regalbuto, J. R., J. Colloid. Interface Sci., 1995, 175, 239.

[26] Babić, B. M. S. K., Milonjic´, B. M. B., Polovina, M. J., Kaludierovi, B. V., Carbon 1999, 37, 477.

[27] Smičklas, I., Dimović, S., Šljivić, M., Plećaš, I., Lončar, B., Mitrić, M., J. Nucl. Mater., 2010, 400, 15.

[28] Pan, X., Wang, J., Zhang, D., Desalination, 2009, 249, 609.

[29] Tóth, J. Adsorption Theory, Modeling, and Analysis, Marcel Dekker, Inc., USA, 2001.

[30] Markhan, E. C., Benton, A. F., J. Am. Chem. Soc., 1931, 53, 497.

[31] Jain, J. S., Snowyink, V. L., J. Water Pollut. Control Fed., 1973, 45, 2463.

[32] Barros, M.A.S.D., Zola A.S., Arroyo, P.A., Sousa-Aguiar, E.F., Tavares, C.R.G., Braz. J. Chem. Eng., 2003, 20, 04, 413.